analytical chemistry

pubs.acs.org/ac Article

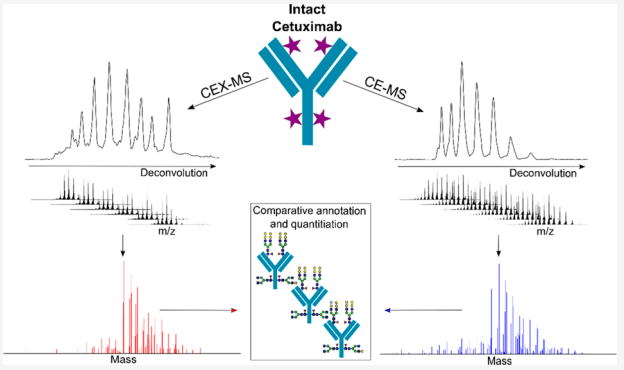
Comparative Elucidation of Cetuximab Heterogeneity on the Intact Protein Level by Cation Exchange Chromatography and Capillary Electrophoresis Coupled to Mass Spectrometry

Florian Füssl, Anne Trappe, Sara Carillo, Craig Jakes, and Jonathan Bones*

Cite This: *Anal. Chem.* 2020, 92, 5431−5438 Read Online

ACCESS | Metrics & More | Article Recommendations | Supporting Information

ABSTRACT: Charge sensitive separation methods such as ion exchange chromatography (CEX) and capillary electrophoresis (CE) have recently been coupled to mass spectrometry to facilitate high resolution profiling of proteoforms present within the charge variant profile of complex biopharmaceuticals. Here we apply pH gradient cation exchange chromatography and microfluidic capillary electrophoresis using the ZipChip platform for comparative characterization of the monoclonal antibody Cetuximab. Cetuximab harbors four glycans per molecule, two on each heavy chain, of which the Fab glycans have been reported to be complex and multiply sialylated. The presence of these extra glycosylation sites in the variable region of the molecule causes significant charge variant and glycan heterogeneity, which makes comprehensive analysis on the intact protein level challenging. Both pH gradient CEX-MS and CE-MS were found to be powerful for the separation of Cetuximab charge variants with eight major peaks being baseline resolved using both separation platforms. Informative native-like mass spectra were collected for each charge variant peak using both platforms that facilitated deconvolution and further analysis. The total proteoform coverage was exceptionally high with >100 isoforms identified and relatively quantified with CEX-MS, in case of CE-MS the proteoform coverage was >200. A deep insight into the heterogeneity of Cetuximab was unveiled, the high level of sensitivity achievable enables the implementation of the presented technologies even at early stages of the biopharmaceutical development platform, such as in developability assessment, process development and also for monitoring process consistency.



Downloaded via MAHASARAKHAM UNIV on July 13, 2020 at 02:43:44 (UTC).
See https://pubs.acs.org/sharingguidelines for options on how to legitimately share published articles.

INTRODUCTION

Cetuximab, a chimeric monoclonal antibody (mAb) targeting the epidermal growth factor receptor (EGFR), was approved for the treatment of metastatic colorectal and head and neck cancer in 2006.[1] Unlike most other therapeutic mAbs, Cetuximab harbors glycosylation not only at the highly conserved site in the Fc region, but also contains an additional N-glycosylation site in the Fab region, leading to increased complexity and heterogeneity of the molecule. Glycosylation of Cetuximab has been studied in the past by released N-glycan analysis,[1,2] middle-up[3−8] and middle-down[9] mass spectrometry, as well as on the glycopeptide level.[10] In contrast to the Fc region which contains the typical core fucosylated biantennary glycans bearing variable galactosylation found on most other mAbs, the Fab region contains murine type glycans, such as alpha 1−3 galactose motifs and N-glycolyl neuraminic acid, which have been shown to increase the risk of elicitation of an immune response upon administration.[11]

The high content of sialic acid present on the N-glycans, together with other modifications of the primary sequence are responsible for a very complex charge variant profile of Cetuximab. Traditional methods used for charge variant profiling of Cetuximab include cation exchange (CEX) chromatography,[12−18] capillary electrophoresis (CE),[5,6,9] and capillary isoelectric focusing (CIEF).[4,19,20] The majority of these studies used UV detection with peak collection following off-line MS analysis if further characterization was performed. A recent report presented an in-depth characterization of Cetuximab heterogeneity employing online CIEF-MS using a middle-up approach. As was also shown in previous studies, the basic Cetuximab charge variants arose from incomplete enzymatic lysine truncation whereas acidic forms were due to the presence of NGNA units on Fab glycans. However, since these experiments were performed solely on protein subunits, the intact protein assembly from differentially

Received: January 15, 2020
Accepted: February 27, 2020
Published: February 27, 2020



© 2020 American Chemical Society

https://dx.doi.org/10.1021/acs.analchem.0c00185
Anal. Chem. 2020, 92, 5431−5438

modified subunits still remains unknown. To this date no reports exist of the comprehensive elucidation of Cetuximab heterogeneity on the intact protein level. Considerable progress has been made over recent years in interfacing previously incompatible separation modes such as ion exchange chromatography to mass spectrometric detection. We recently introduced a pH gradient CEX-MS method for the online mass spectrometric characterization of charge variants of multiple monoclonal antibodies.[16] This method was further optimized for the analysis of Cetuximab as described herein, with a focus on separation selectivity and the quality of the MS response, yielding eight well resolved Cetuximab charge variant peaks of varying abundance, each containing highly informative native mass spectra, which enabled deep annotation of the proteoforms present in each peak. In addition we also explored the potential of the ZipChip microfluidic CE-MS technology, which has proven powerful for a variety of biopharma-related applications including intact native protein characterization.[21−26] Using CE-MS we obtained a similar charge variant distribution with eight clearly distinguishable peaks, however, with different separation selectivity. Both approaches resulted in the generation of native-like protein spectra without any sign of protein denaturation, albeit showing a difference in the number of charge states observed due to differences in the separation mechanisms and also additives present in the background electrolyte used on the CE-MS system.

Isoform annotation was supported by glycopeptide mapping and revealed good intermethod correlation with respect to the type and relative abundance of Cetuximab species found. Basic variants were found to be due to the presence of up to two unprocessed C-terminal lysine residues, whereas acidic peaks contained variants with up to five NGNA residues. For the CE-MS separation, a size distribution of isoforms within individual charge variant peaks was observed revealing varying migration times dependent on the size and complexity of the Fab glycans. Both methodologies appear powerful for the analysis of complex mAbs on the intact protein level revealing more than 100 different isoforms mapped by either technique.

Mass spectrometry is advancing and is becoming more and more powerful for the characterization of biopharmaceuticals, also increasingly showing potential for implementation in GMP environments.[27−29] Highly informative analytical methods can be of enormous benefit, especially in stages like developability assessment, often performed in combination with forced degradation studies, or comparability testing, but have also proven valuable in later stages such as batch release testing.[29−33] Having demonstrated great potential for intact protein characterization, both CEX-MS and CE-MS can be considered cutting-edge, highly informative analytical characterization techniques which can be applied within and possibly even transform the biopharmaceutical development and manufacturing pipeline of the present.

MATERIAL AND METHODS

Chemicals and Materials. Ultrapure water (Optima, LC-MS grade) was provided by Fisher Scientific (Dublin, Ireland). Ammonium bicarbonate (≥99.5%), acetic acid (≥99.7%), ammonium hydroxide (BioUltra, 1 M in H_2O), DL-dithiothreitol, and iodoacetamide were purchased from Sigma-Aldrich (Wicklow, Ireland). Amicon Ultra-0.5 mL centrifugal filters with a cutoff size of 10 kDa were obtained from Merck (Tullagreen, Ireland). ZipChip HRN chips and the Native Antibodies Kit for ZipChip analysis were obtained from 908 devices (Boston, MA). The monoclonal antibody Cetuximab was obtained from the Hospital Pharmacy Unit of the University Hospital of San Cecilio (Granada, Spain).

Sample Preparation. For CEX-MS intact Cetuximab was directly injected in formulation buffer. For CE-MS the mAb was buffer exchanged to native antibody sample diluent provided by 908 devices using Amicon Ultra-0.5 mL centrifugal filters to obtain a final concentration of 1 mg/mL. For peptide mapping experiments Cetuximab was digested using KingFisher SMART digestion as previously described.[16] After digestion peptides were reduced in 10 mM DTT at 57 °C for 30 min and alkylated in 20 mM iodoacetamide for 30 min at room temperature in the dark. Injection amount was 5 μg of protein on column.

pH-Gradient CEX-MS and Microfluidic CE-MS Analysis. pH-gradient CEX-MS analysis was performed on a Thermo Scientific Vanquish Flex UHPLC system interfaced to a Thermo Scientific Q Exactive hybrid quadrupole Orbitrap mass spectrometer equipped with the extended mass BioPharma option. The chromatographic buffer A was 6.25 mM ammonium bicarbonate and 7.5 mM acetic acid in water (pH 5.40) and chromatographic buffer B was 5 mM ammonium hydroxide in water (pH 9.85). Separation of Cetuximab was performed with a linear gradient of 20−100% buffer B in 15 min followed by 3 min of column flushing at 100% buffer B, 3 min equilibration to 0% buffer B and 12 min equilibration to the starting conditions of 20% buffer B. One hundred μg protein were injected on column. All other run parameters used for analysis were as previously described.[18] CE-MS analysis was performed on a HRN chip via the ZipChip interface coupled to a Q Exactive Plus instrument with extended mass Biopharma Option and a model 840 autosampler provided by 908 devices. Injection volume was 2 nL of a 1 mg/mL Cetuximab solution in native sample diluent, background electrolyte was native antibodies BGE prepared following the ZipChip protocol *Boosting Sensitivity for Intact Antibody Charge Variant Analysis*,[34] initial field strength was 500 V/cm, pressure assist start time was 0.5 min and analysis time was 16 min. MS acquisition was performed in HMR mode, scan range was 2500−8000 m/z, In-source CID was 125 eV, the resolution setting was 35 000, the polarity was positive, the number of microscans was 10, the AGC target 1e6, the maximum inject time 10 ms, the sheath gas flow rate was 2 arbitrary units, the capillary temperature 250 °C and the S-lens RF level 200. Cetuximab was analyzed in triplicate with both methods.

Data Analysis. Deconvolution of intact raw files was performed using the Sliding Window feature in BioPharma Finder 3.0. (Thermo Fisher Scientific). Deconvolution mass tolerance was 12 ppm, model mass range was 150 000−156 000, charge state range was 20−30, minimum adjacent charges were 3 to 3, and target mass was 153 000. Deconvolution was performed of triplicate data files, multi-consensus component merge mass tolerance was 20 ppm, and RT tolerance was 0.1 and 0.05 min for CEX-MS and CE-MS, respectively. For sliding window deconvolution of CEX-MS files a target average spectrum width of 0.2 min, a target average spectrum offset of 1, a merge tolerance of 12 ppm, a max RT gap of 0.2 min, and a minimum number of detected intervals of 3 was set. The same parameters for the CE-MS files were 0.1 min, 1, 12 ppm, 0.1 min, and 3, respectively. For both methods, only species found in all three replicate runs were

https://dx.doi.org/10.1021/acs.analchem.0c00185
Anal. Chem. 2020, 92, 5431−5438

considered for annotation. Also the analysis of peptide mapping data was performed in BioPharma Finder 3.0. The protein sequence[3] was introduced together with the following modifications: Carbamidomethylation of C, pyroglutamate formation of Q, deamidation of N, oxidation of M and C, N-glycosylation (CHO), and isomerization of D. As enzyme trypsin was chosen with high specificity for K and R, and the minimum confidence score was set to 0.8. Annotation was supported by the MoFi software after introduction of the protein sequence, and modifications such as c-terminal lysine, succinimide, and glycosylation.[35] For probability based assignments of isoforms, the type and relative abundance of glycans obtained by peptide mapping were introduced and annotation was performed within a mass tolerance of ±50 ppm. In cases where more than 1 possible hit was reported, the one with the highest hit score was accepted under the premise that the set of charge altering modifications was coherent with regard to the retention/migration time. The glycan nomenclature used throughout this manuscript is the same as is given by the BioPharma Finder 3.0 software.

RESULTS AND DISCUSSION

Evaluation and Comparison of Charge Variant Separations. Cetuximab is a monoclonal antibody with high charge variant heterogeneity, resulting in complex chromatograms and electropherograms during charge variant profiling. Figure 1 shows the resulting chromatogram and electropherogram obtained with pH gradient CEX-MS and microfluidic CE-MS, respectively. Both separations initially appear visually comparable with regard to the number of separated features, however, investigation of the data confirmed reversed elution order of acidic and basic variants, as expected, based on the different underlying separation mechanisms. In pH gradient CEX-MS charge variants elute in order of increasing isoelectric point, in CE-MS migration time is positively correlated with increasing negative charge and hence, slower electrophoretic mobility of the variant ions under the applied field. As can be seen in Figure 1 both, CEX and CE of Cetuximab yielded the separation of eight charge variant peaks. Comparing elution time window and peak width, CE-MS was found to generate sharper peaks eluting within a ∼4 min separation window versus an ∼10 min separation window in case of pH gradient CEX-MS. As mass spectrometric detection was desired, it was necessary to consider the average peak width to ensure sufficient time for acquisition of an adequate number of mass spectra per peak. Both methods were found to fulfill this criterion, although the comparatively narrow peaks obtained via CE-MS required different parameter settings in terms of MS data acquisition and deconvolution. An additional difference observed was that the peak width using pH gradient CEX-MS was constant throughout the gradient while it steadily increased across the electropherogram, which is attributed to the different nature of the two separation mechanisms. The electropherogram also contained lower background noise than the chromatogram which is likely related to the significantly lower operational flow rate of the microfluidic CE-MS device and, therefore, more efficient droplet desolvation during the ESI process.

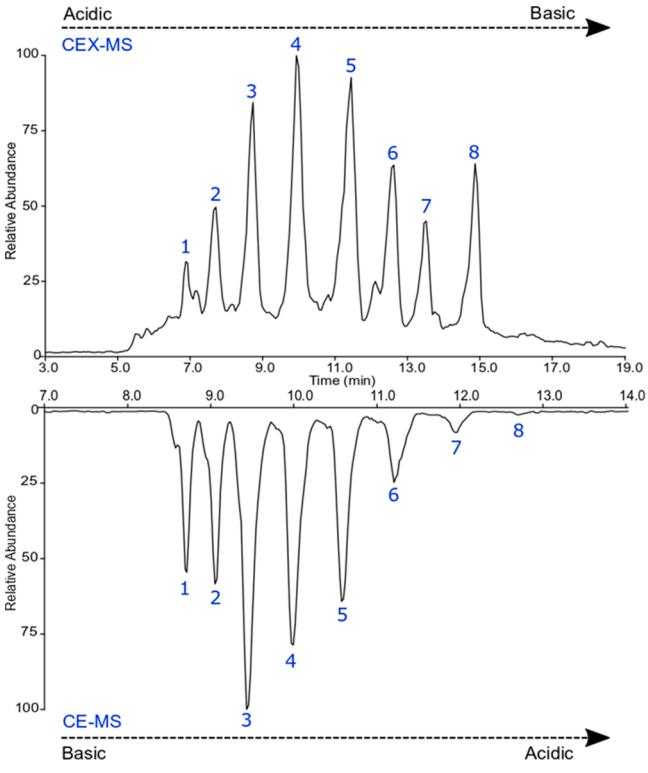


Figure 1. Comparison of the separations obtained via CEX-MS and CE-MS. The top panel shows the base peak chromatogram, whereas the bottom panel displays the base peak electropherogram. Main peaks are numbered from 1 to 8, and the elution order is indicated by the labeled arrows.

MS Spectral Comparison and Evaluation of Spectral Features Post Deconvolution. Figure 2A shows the charge envelopes obtained after spectral averaging of the main charge variant peak of both separations, respectively. Both envelopes are of excellent quality and are centered at a mass range of ∼6000 m/z, clearly inferring preservation of the native molecular state. For better visualization only the m/z region of interest is shown; however, the lower m/z region does not contain any sign of denatured protein in either case (Supporting Information (SI) Figure S1). While the most abundant charge states in both spectra are the same, the general width of the charge envelope distribution is subject to considerable variation. In case of CEX-MS, 5−6 charge states are observable, whereas CE-MS-based spectra shows a broader distribution with approximately 11 clearly discernible species. The most probable reason for this observed difference is the presence of dimethyl sulfoxide (DMSO) in the background electrolyte used for CE-MS, which is not present in the mobile phases used for CEX-MS. Depending on the concentration of DMSO, intact proteins may become more compact or may relax, thereby resulting in lower charged species in the former case and in higher charge states for the same protein in the latter.[36] The extension of the charge envelope observed in CE-MS in both directions suggests that the concentration of DMSO in the background electrolyte promotes an equilibrium of both effects, compaction and relaxation of the protein structure at the same time and to a limited extent.

Even though the number of charge states observable is different, the spectral heterogeneity and information content appears to be the same, as is shown in Figure 2A in the right-hand panel.

Deconvolution of triplicate pH gradient CEX-MS and CE-MS data files was performed using the Sliding Window feature of the BioPharma Finder software. The total yield in proteoforms found across the replicate measurements was

https://dx.doi.org/10.1021/acs.analchem.0c00185
Anal. Chem. 2020, 92, 5431−5438

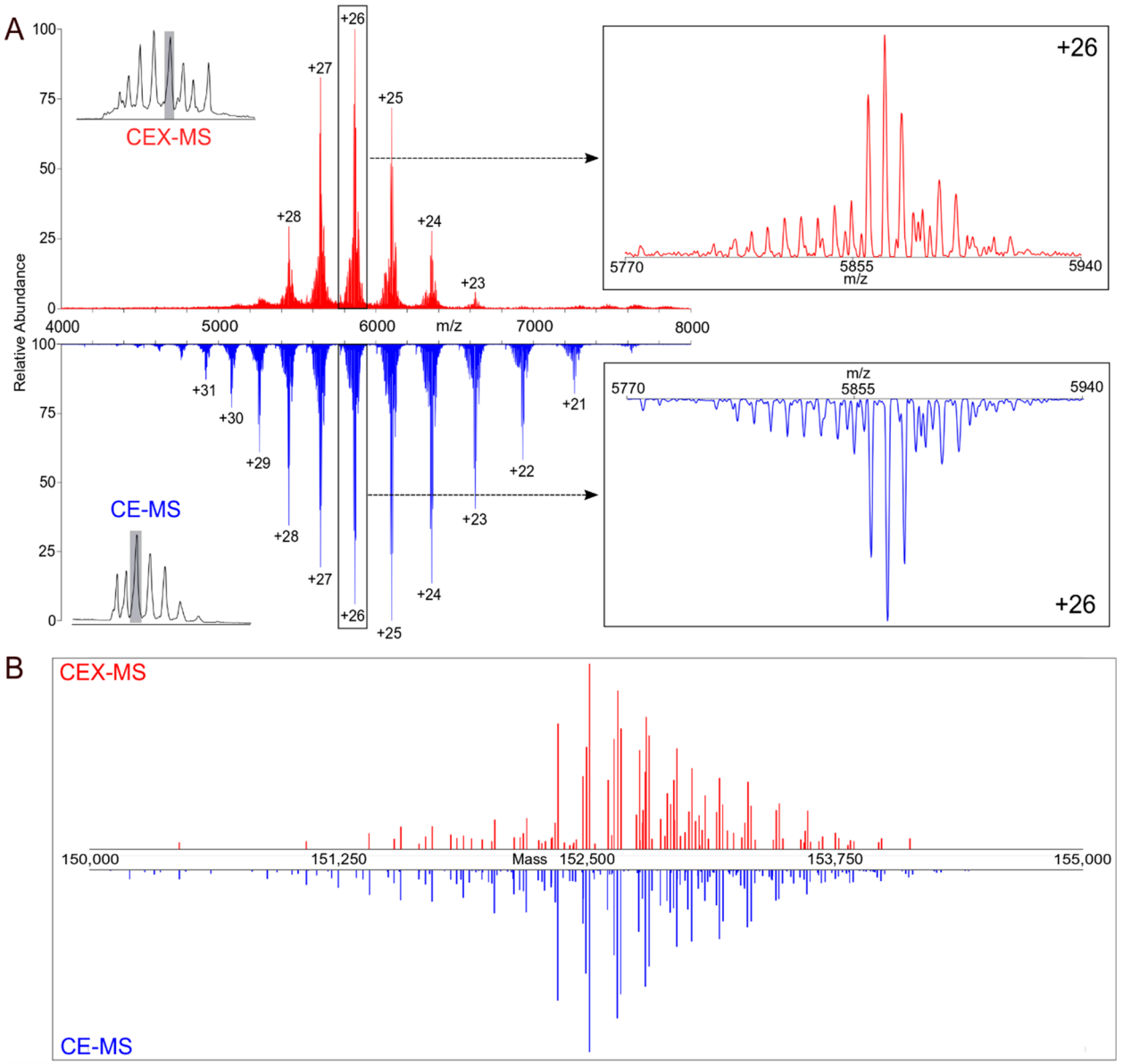


Figure 2. (A) Comparison of the charge envelopes obtained by the two orthogonal analytical approaches after spectral averaging of the main charge variant peaks which are labeled in gray in the left panel. The charge states are indicated in black. Charge state +26 is magnified and shown in the right panel for enhanced visualization of the glycoform heterogeneity. (B) Comparison of deconvoluted spectra from CEX-MS and CE-MS analysis. The CEX-MS spectra are represented in red, while the CE-MS derived spectra are shown in blue.

109 and 218 species for pH gradient CEX-MS and CE-MS analysis, respectively. Figure 2B shows a comparison of the complex deconvoluted spectra obtained for both approaches, representing all species found across the whole elution/migration time. The spectra obtained resemble each other well, showing good alignment in the type and relative abundance of species found. However, several low abundant species found via CE-MS were not seen in CEX-MS data files, demonstrating improved sensitivity achievable using the microfluidic CE-MS device and its lower operational flow rate.

Charge Variant−Elution/Migration Time Relationship and Cetuximab Isoform Annotation. Glycans on mAbs are composed of only very few different monosaccharides, some of which are isobaric. This makes an unambiguous assignment of intact Cetuximab isoforms, in terms of glycan composition and distribution, extremely challenging.

To partially overcome this problem Cetuximab isoform annotation was performed using site specific glycopeptide data generated by peptide mapping. Figure 3 shows an overview over all glycans found for the Cetuximab Fc and Fab region. The Fc region is occupied by rather simple glycans such as A2G0F and A2G1F, which are commonly found on IgG's. The Fab region is in contrast dominated by biantennary, more complex glycans such as A2Ga2F. In terms of relative abundance these are being followed by sialylated forms, simpler biantennary glycans and larger triantennary structures.

The fractional abundance of the glycans present at each glycosylation site as determined using peptide mapping was then used as an input for MoFi, a software previously reported for annotation of complex intact protein mass spectra.[35] MoFi returned a list with possible hits for each deconvoluted mass within a defined mass accuracy window and a Hit Score representing their likelihood of being correct. For each mass,

https://dx.doi.org/10.1021/acs.analchem.0c00185
Anal. Chem. 2020, 92, 5431−5438

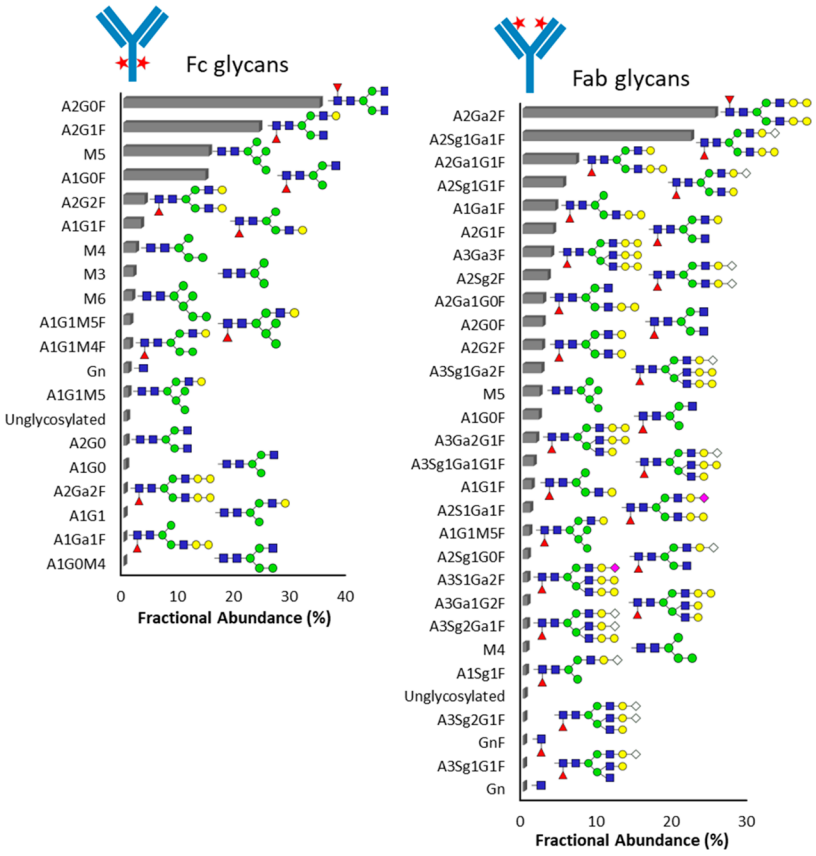


Figure 3. List of Cetuximab Fc and Fab glycans shown in order of decreasing fractional abundance from top to bottom. The data shown is based on peptide mapping experiments. For all glycans the nomenclature, as is used by the Thermo Fisher Scientific BioPharma Finder 3.0 software, as well as structures are shown.

the assignment with the best hit score was considered the actual positive hit, with the requirement of noncharge altering modifications being consistent across charge variant peaks. Moreover, hits had to be coherent with regard to the expected net charge based on number of acidic and basic modifications and their retention or migration times. Importantly, according to peptide mapping data, there is not only one but more possibilities for arranging glycans on Cetuximab in order to align with the intact molecular masses obtained. In consequence, it is likely that many MS peaks correspond to more than one Cetuximab isoform. To simplify matters, the only variants reported are those which are most probable based on fractional abundances derived from peptide mapping data. For each annotation the possible number of permutations is reported as well.

Cetuximab charge variant analysis was started by the investigation of patterns across and within the charge variant peaks. In this course it was observed that spectral complexity and the MS peak pattern observed were highly conserved between peaks with the only difference of showing distinct mass offsets shifting the spectra along the mass axis. Basic peaks, for example, showed a positive mass offset of one and two times 128 Da, respectively, when compared to the main peak. This suggests that basic charge variants are caused by insufficient C-terminal lysine residue processing, which also correlates well to a later or earlier elution in CEX-MS and CE-MS, respectively. Acidic peaks showed positive mass offsets of up to 5 times 145 Da when compared to the main peak. This offset was not directly indicative of the mass of an additional residue but rather represents the mass difference between a galactose and a N-glycolyl neuraminic acid unit. This is in agreement with previous studies revealing that Cetuximab charge variant heterogeneity is caused by various degrees of nontruncated C-terminal lysine residues and sialylation, yielding the characteristic separation profiles observed. Figure 4A depicts the chromatogram and electropherogram with major charge variant peaks labeled in red according to increasing retention/migration times and in blue according to their net charge dependent on the number of C-terminal lysine residues and NGNA units present. In total eight major peaks can be distinguished in each separation, and the total number of net charges ranges from +2 to −4 in case of CEX-MS and +2 to −5 for CE-MS. Figure 4B shows the averaged deconvoluted mass spectra obtained for each peak. The labeling is according to Figure 4A, and peaks from the two different data sets corresponding to the same charge variant are horizontally aligned. The spectra of seven charge variant peaks correspond well between chromatogram to electropherogram, which is indicated by a high spectral similarity. The set of charge altering modifications each spectrum is representing is shown in blue in Figure 4B. Notably this only represents the major set of modifications, spectra can also contain species with a higher number of modifications, which, however, result in the same net charge. Most spectra shown are dominated by three MS peaks corresponding to Cetuximab with the Fc glycan pairs A2G0F/A2G0F, A2G0F/A2G1F, and A2G1F/A2G1F, while the Fab region is occupied by more complex biantennary glycan pairs such as A2Ga2F/A2Ga2F. In case of

https://dx.doi.org/10.1021/acs.analchem.0c00185
Anal. Chem. 2020, 92, 5431−5438

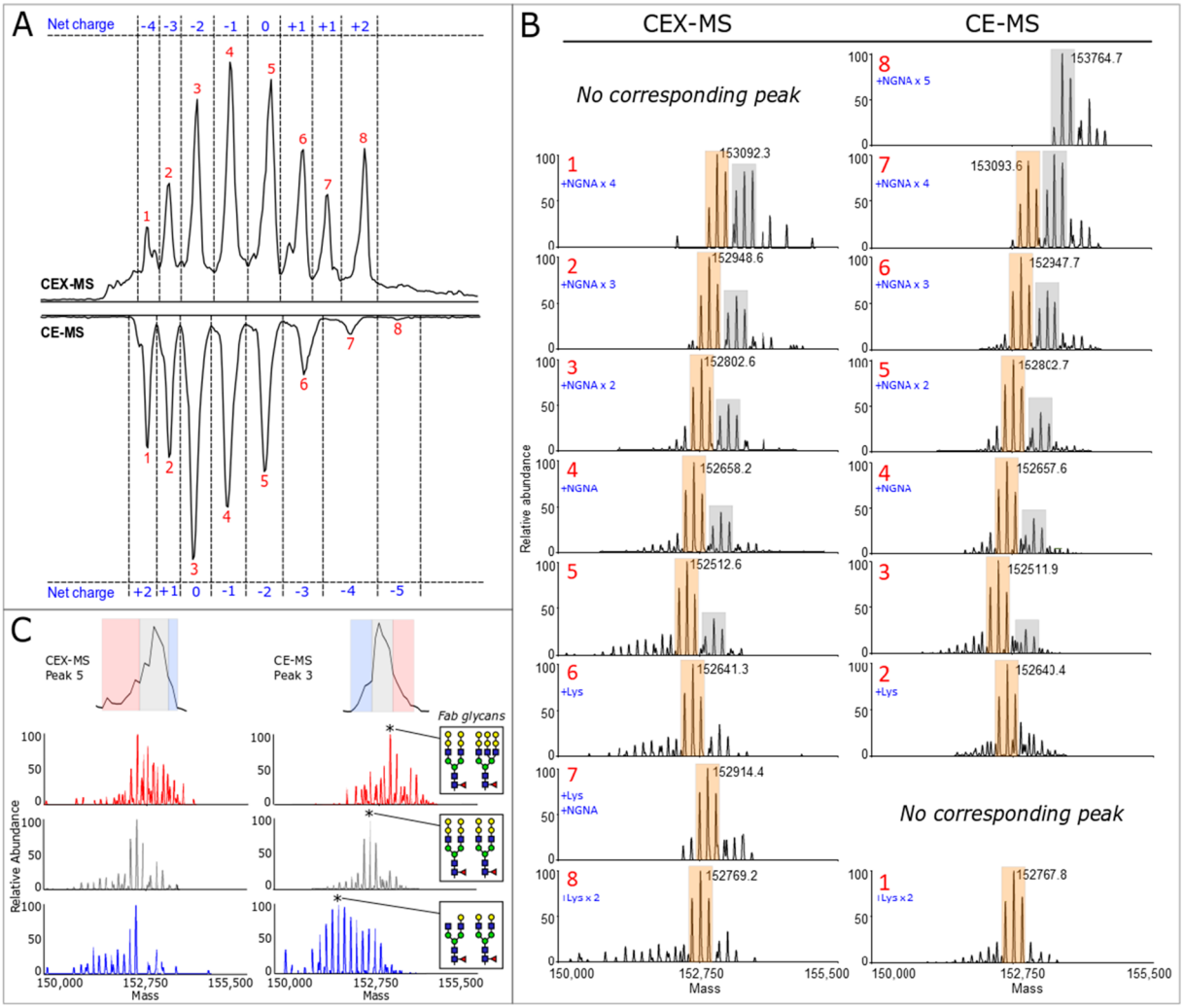


Figure 4. (A) Cetuximab chromatogram and electropherogram. Peaks are labeled in red in order of increasing retention/migration time. The net charge is represented in blue. (B) Deconvoluted averaged mass spectra corresponding to each peak. Spectra from the two separation approaches containing the same charge variant species are aligned horizontally. Peak assignment is based on the corresponding red labels in panel A. Modifications that are causing differences in the net charge are indicated in blue, whereas only the most probable combination of modifications is given. The most abundant species corresponding to biantennary Fab glycan pairs are shown in orange, whereas the most abundant forms carrying triantennary Fab glycans are labeled in gray. (C) Deconvoluted spectra of peak front, center, and tail of peaks 5 and 3 of the CEX and CE separation, respectively. Associated spectra are aligned horizontally and are shown in the same color.

more acidic charge variant peaks the terminal galactose units of the Fab glycans are successively replaced by NGNA units, slightly decreasing the protein pI while increasing protein mass. These species are highlighted in orange throughout the spectra shown. The most abundant species of each spectrum is also labeled with the respective molecular weight to provide the basis for tracing back the characteristic mass shifts observed. Another distribution which is labeled in gray in Figure 4B can be observed especially for the acidic charge variant peaks in the higher mass range. These species contain the same Fc glycan pairs but are higher in mass as they contain larger triantennary glycans in the Fab region. Their relative abundance compared to the double biantennary Fab glycan species is increasing together with the negative net charge of the charge variant peaks and is highest in peak 8 of the CE-MS separation. In this spectrum no double biantennary Fab glycan species are being observed since at least one triantennary glycan is required to yield a total NGNA number of five. These highly sialylated species were not found in the CEX-MS run, presumably due to differential method sensitivity.

Peak 7 of the CEX-MS separation was in contrast not observed in the electropherogram (Figure 4A and B). The species contained within are corresponding to Cetuximab variants modified with 2 C-terminal lysine residues and 1 sialylation which apparently are separated from variants solely modified with one C-terminal lysine residue. In the CE-MS raw data these species are not separated and can be found all together within peak 2. Another less noticeable difference is represented by a minor shoulder of peak 6 of the CEX-MS run. This peak corresponds to variants modified by two C-terminal lysine residues and two NGNA residues. These species also do not appear as a separate peak in the electropherogram and are contained within peak 3. Species within peak 8 of the electropherogram were solely found in case of CE-MS. An analysis of the molecular weight and retention time indicated the presence of glycans with three NGNA units attached. Together with a second Fab glycan carrying two NGNA's the

https://dx.doi.org/10.1021/acs.analchem.0c00185
Anal. Chem. 2020, 92, 5431−5438

total net charge of these isoforms is −5. Triply sialylated glycans were also not found via peptide mapping, thus annotation in these cases was performed manually. The two methods compared also behave differently regarding the distribution of isoforms throughout individual charge variant peaks. The deconvoluted spectra of the front, center, and tail of the main peaks 5 and 3, respectively, are shown in Figure 4C. The different regions of the CEX-MS peak look similar, whereas those of the CE-MS peak only poorly resemble each other. Closer investigation revealed that the peak front of the CE-MS peak contains lower molecular weight isoforms corresponding to species with simple and rather small Fab glycan pairs (Figure 4C, blue trace). The central region of the peak predominantly contains larger biantennary Fab glycan pairs (Figure 4C, gray trace) and the peak tail a higher portion of variants with large triantennary Fab glycans (Figure 4C, red trace). Possessing the same net charge, these different species are likely separated due to their different Fab glycan size going along with a differential hydrodynamic radius. Hence, the presence of smaller glycans is probably causing an increase in the molecular migration velocity going along with earlier migration times, whereas the opposite is true for larger glycans. This behavior is not seen in CEX as the elution time is in this case solely depends on the protein net charge. A full, comprehensive table of all Cetuximab variants found for both approaches is shown in the SI Tables S-1 and S-2.

CONCLUSIONS

The monoclonal antibody Cetuximab was subject of an in-depth analysis in terms of charge variant and glycoform heterogeneity using two orthogonal approaches, cation exchange chromatography, and capillary electrophoresis, both directly interfaced to mass spectrometry. Albeit showing slight differences in terms of separation selectivity, both approaches have proven powerful for the separation of Cetuximab charge variants resulting in the separation of eight main charge variant peaks with either approach. In terms of MS spectral quality, both techniques clearly allow for the generation of native-like mass spectra evidently well suitable for deconvolution and further analysis.

The results of both analyses show that acidic Cetuximab charge variants are caused by various levels of sialylation of the Fab glycans with predominantly N-glycolylneuraminic acid. Basic variants are in turn derived by incomplete C-terminal lysine residue processing and charge variant peaks represent specific net charge states caused by various combinations of these two types of modifications. Cetuximab isoforms found are diverse, ranging from lower molecular weight variants with very simple glycans and no sialic acids to forms with multiple triantennary glycans in the Fab region which can also be multiply sialylated. In addition to charge variant separation, CE-MS also facilitated a hydrodynamic radius-dependent separation of species based on different glycoform complexity within individual charge variant peaks.

In total 109 and 218 isoforms were found via CEX-MS and CE-MS, respectively. Differential sensitivity with lower sample consumption was achieved based on the lower operational flow rate and the presence of DMSO in the background electrolyte used for CE-MS. CEX-MS appeared to be less susceptible to interferences caused by drug formulations and more versatile as it can easily be combined with other detection modes such as UV detection if desired. Additionally, CEX-MS allows for optimization and manipulation of run parameters such as buffer strength or gradient length and slope. Nevertheless, in contrast to CEX-MS, CE-MS does not require individual method optimization for a particular mAb as the run parameters employed appear to be suitable for the charge variant analysis of conventional mAbs. With sample consumption of only ∼1 ng and an operational flow rate in the low nL-range, the application of CE-MS shows great potential, especially in early stages of the biopharmaceutical process pipeline, where high method sensitivity is imperative. CEX-MS, in contrast, operates at a higher flow and has higher sample consumption making it attractive for the application in later states of the development pipeline, such as in batch release testing.

ASSOCIATED CONTENT

Supporting Information

The Supporting Information is available free of charge at https://pubs.acs.org/doi/10.1021/acs.analchem.0c00185.

Averaged mass spectra of the main Cetuximab charge variant peaks of a CEX-MS and CE-MS data file, respectively, (p S2); list of all Cetuximab forms found via CEX-MS analysis, (pp S3−S5); list of all Cetuximab forms found via CE-MS analysis, (pp S6−S10) (PDF)

AUTHOR INFORMATION

Corresponding Author

Jonathan Bones − *NIBRT − The National Institute for Bioprocessing Research and Training, Dublin A94 X099, Ireland; School of Chemical and Bioprocess Engineering, University College Dublin, Dublin D04 V1W8, Ireland;* orcid.org/0000-0002-8978-2592; Phone: +353 1215 8100; Email: jonathan.bones@nibrt.ie; Fax: +353 1215 8116

Authors

Florian Füssl − *NIBRT − The National Institute for Bioprocessing Research and Training, Dublin A94 X099, Ireland*

Anne Trappe − *NIBRT − The National Institute for Bioprocessing Research and Training, Dublin A94 X099, Ireland*

Sara Carillo − *NIBRT − The National Institute for Bioprocessing Research and Training, Dublin A94 X099, Ireland*

Craig Jakes − *NIBRT − The National Institute for Bioprocessing Research and Training, Dublin A94 X099, Ireland; School of Chemical and Bioprocess Engineering, University College Dublin, Dublin D04 V1W8, Ireland*

Complete contact information is available at: https://pubs.acs.org/10.1021/acs.analchem.0c00185

Notes

The authors declare no competing financial interest.

ACKNOWLEDGMENTS

We gratefully acknowledge 908 devices and Thermo Fisher Scientific for instrument access and support and the Science Foundation of Ireland for funding (Grant No. 13/CDA/2196). We also want to thank Dr. Wolfgang Esser-Skala from the Christian Doppler Laboratory for Innovative Tools for Biosimilar Characterization at the University of Salzburg, Austria for software support.

https://dx.doi.org/10.1021/acs.analchem.0c00185
Anal. Chem. 2020, 92, 5431−5438

REFERENCES

(1) Qian, J.; Liu, T.; Yang, L.; Daus, A.; Crowley, R.; Zhou, Q. W. *Anal. Biochem.* **2007**, *364*, 8−18.
(2) Wiegandt, A.; Meyer, B. *Anal. Chem.* **2014**, *86*, 4807−4814.
(3) Ayoub, D.; Jabs, W.; Resemann, A.; Evers, W.; Evans, C.; Main, L.; Baessmann, C.; Wagner-Rousset, E.; Suckau, D.; Beck, A. *MAbs* **2013**, *5*, 699−710.
(4) Dai, J.; Zhang, Y. *Anal. Chem.* **2018**, *90*, 14527−14534.
(5) Francois, Y. N.; Biacchi, M.; Said, N.; Renard, C.; Beck, A.; Gahoual, R.; Leize-Wagner, E. *Anal. Chim. Acta* **2016**, *908*, 168−176.
(6) Biacchi, M.; Gahoual, R.; Said, N.; Beck, A.; Leize-Wagner, E.; Francois, Y. N. *Anal. Chem.* **2015**, *87*, 6240−6250.
(7) D'Atri, V.; Fekete, S.; Beck, A.; Lauber, M.; Guillarme, D. *Anal. Chem.* **2017**, *89*, 2086−2092.
(8) Sorensen, M.; Harmes, D. C.; Stoll, D. R.; Staples, G. O.; Fekete, S.; Guillarme, D.; Beck, A. *MAbs* **2016**, *8*, 1224−1234.
(9) Biacchi, M.; Said, N.; Beck, A.; Leize-Wagner, E.; Francois, Y. N. *J. Chromatogr A* **2017**, *1498*, 120−127.
(10) Gahoual, R.; Biacchi, M.; Chicher, J.; Kuhn, L.; Hammann, P.; Beck, A.; Leize-Wagner, E.; Francois, Y. N. *MAbs* **2014**, *6*, 1464−1473.
(11) Chung, C. H.; Mirakhur, B.; Chan, E.; Le, Q. T.; Berlin, J.; Morse, M.; Murphy, B. A.; Satinover, S. M.; Hosen, J.; Mauro, D.; Slebos, R. J.; Zhou, Q.; Gold, D.; Hatley, T.; Hicklin, D. J.; Platts-Mills, T. A. *N. Engl. J. Med.* **2008**, *358*, 1109−1117.
(12) Fekete, S.; Beck, A.; Guillarme, D. *J. Pharm. Biomed. Anal.* **2015**, *111*, 169−176.
(13) Fekete, S.; Beck, A.; Fekete, J.; Guillarme, D. *J. Pharm. Biomed. Anal.* **2015**, *102*, 282−289.
(14) Fekete, S.; Beck, A.; Fekete, J.; Guillarme, D. *J. Pharm. Biomed. Anal.* **2015**, *102*, 33−44.
(15) Hintersteiner, B.; Lingg, N.; Janzek, E.; Mutschlechner, O.; Loibner, H.; Jungbauer, A. *Biotechnol. J.* **2016**, *11*, 1617−1627.
(16) Fussl, F.; Cook, K.; Scheffler, K.; Farrell, A.; Mittermayr, S.; Bones, J. *Anal. Chem.* **2018**, *90*, 4669−4676.
(17) Trappe, A.; Fussl, F.; Carillo, S.; Zaborowska, I.; Meleady, P.; Bones, J. *J. Chromatogr. B: Anal. Technol. Biomed. Life Sci.* **2018**, *1095*, 166−176.
(18) Fussl, F.; Trappe, A.; Cook, K.; Scheffler, K.; Fitzgerald, O.; Bones, J. *MAbs* **2019**, *11*, 116−128.
(19) Dai, J.; Lamp, J.; Xia, Q.; Zhang, Y. *Anal. Chem.* **2018**, *90*, 2246−2254.
(20) Kinoshita, M.; Nakatsuji, Y.; Suzuki, S.; Hayakawa, T.; Kakehi, K. *J. Chromatogr A* **2013**, *1309*, 76−83.
(21) Giorgetti, J.; Lechner, A.; Del Nero, E.; Beck, A.; Francois, Y. N.; Leize-Wagner, E. *Eur. J. Mass Spectrom.* **2019**, *25*, 324−332.
(22) Kelley, Z. D.; Rogers, D. T.; Littleton, J. M.; Lynn, B. C. *Electrophoresis* **2019**, *40*, 2921−2928.
(23) Beri, J.; Kirkwood, K. I.; Muddiman, D. C.; Bereman, M. S. *Anal. Bioanal. Chem.* **2018**, *410*, 2597−2605.
(24) Khatri, K.; Klein, J. A.; Haserick, J. R.; Leon, D. R.; Costello, C. E.; McComb, M. E.; Zaia, J. *Anal. Chem.* **2017**, *89*, 6645−6655.
(25) Redman, E. A.; Batz, N. G.; Mellors, J. S.; Ramsey, J. M. *Anal. Chem.* **2015**, *87*, 2264−2272.
(26) Redman, E. A.; Mellors, J. S.; Starkey, J. A.; Ramsey, J. M. *Anal. Chem.* **2016**, *88*, 2220−2226.
(27) Rathore, D.; Faustino, A.; Schiel, J.; Pang, E.; Boyne, M.; Rogstad, S. *Expert Rev. Proteomics* **2018**, *15*, 431−449.
(28) Rogstad, S.; Yan, H.; Wang, X.; Powers, D.; Brorson, K.; Damdinsuren, B.; Lee, S. *Anal. Chem.* **2019**, *91*, 14170−14177.
(29) Sokolowska, I.; Mo, J.; Rahimi Pirkolachahi, F.; McVean, C.; Meijer, L. A. T.; Switzar, L.; Balog, C.; Lewis, M. J.; Hu, P. *Anal. Chem.* **2020**, *92*, 2369−2373.
(30) Xu, Y.; Wang, D.; Mason, B.; Rossomando, T.; Li, N.; Liu, D.; Cheung, J. K.; Xu, W.; Raghava, S.; Katiyar, A.; Nowak, C.; Xiang, T.; Dong, D. D.; Sun, J.; Beck, A.; Liu, H. *MAbs* **2019**, *11*, 239−264.
(31) Nowak, C.; Cheung, J. K.; Dellatore, S. M.; Katiyar, A.; Bhat, R.; Sun, J.; Ponniah, G.; Neill, A.; Mason, B.; Beck, A.; Liu, H. *MAbs* **2017**, *9*, 1217−1230.
(32) Halley, J.; Chou, Y. R.; Cicchino, C.; Huang, M.; Sharma, V.; Tan, N. C.; Thakkar, S.; Zhou, L. L.; Al-Azzam, W.; Cornen, S.; Gauden, M.; Gu, Z.; Kar, S.; Lazar, A. C.; Mehndiratta, P.; Smith, J.; Sosic, Z.; Weisbach, P.; Stokes, E. S. E. *J. Pharm. Sci.* **2020**, *109*, 6−21.
(33) Ambrogelly, A.; Gozo, S.; Katiyar, A.; Dellatore, S.; Kune, Y.; Bhat, R.; Sun, J.; Li, N.; Wang, D.; Nowak, C.; Neill, A.; Ponniah, G.; King, C.; Mason, B.; Beck, A.; Liu, H. *MAbs* **2018**, *10*, 513−538.
(34) 908devices, Boosting Sensitivity for Intact Antibody Charge Variant Analysis: https://908devices.zendesk.com, 2019.
(35) Skala, W.; Wohlschlager, T.; Senn, S.; Huber, G. E.; Huber, C. G. *Anal. Chem.* **2018**, *90*, 5728−5736.
(36) Sterling, H. J.; Prell, J. S.; Cassou, C. A.; Williams, E. R. *J. Am. Soc. Mass Spectrom.* **2011**, *22*, 1178−1186.

https://dx.doi.org/10.1021/acs.analchem.0c00185
Anal. Chem. 2020, 92, 5431−5438